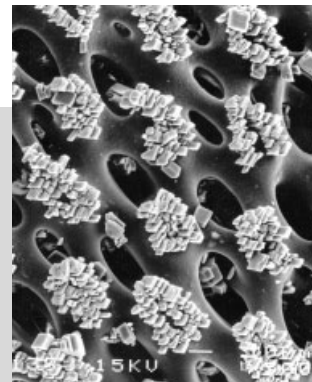


# Crystallization in Patterns: A Bio-Inspired Approach\*\*

By Joanna Aizenberg\*

*Nature produces a wide variety of exquisite, highly functional mineralized tissues using simple inorganic salts. Biomineralization occurs within specific microenvironments, and is finely tuned by cells and specialized biomacromolecules. This article surveys bio-inspired approaches to artificial crystallization based on the above concept: that is, the use of organized organic surfaces patterned with specific initiation domains on a sub-micrometer scale to control patterned crystal growth. Specially tailored self-assembled monolayers (SAMs) of  $\omega$ -terminated alkanethiols were micropatterned on metal films using soft lithography and applied as organic templates for the nucleation of calcium carbonate. Crystallization results in the formation of large-area, high-resolution inorganic replicas of the underlying organic patterns. SAMs provide sites for ordered nucleation, and make it possible to control various aspects of the crystallization process, including the precise localization of particles, nucleation density, crystal sizes, crystallographic orientation, morphology, polymorph, stability, and architecture. The ability to construct periodic arrays of uniform oriented single crystals, large single crystals with controlled microporosity, or films presenting patterns of crystals offers a potent methodology to materials engineering.*



## 1. Technological Challenge and Biological Inspiration

The ability to control crystallization is a critical requirement in the synthesis of many technologically important materials.<sup>[1–5]</sup> Crystalline inorganic structures with micrometer-scale regularity have applications in microelectronics, optics, information storage, biomedical implants, catalysis, and separation technologies.<sup>[6–9]</sup> Such patterned crystalline materials are currently manufactured in a top-down fashion—a multi-step process involving the growth of a bulk single crystal, its cutting and polishing in preferred crystallographic orientations, followed by patterning procedures that include the “writing” of desired patterns on the surface using lithographic techniques and their engraving into the crystal using various etching procedures.<sup>[10,11]</sup>

Of the many challenges facing materials science, the development of an alternative, bottom-up crystallization route, which would enable the direct, patterned growth of crystals with controlled physico-chemical properties, became an attractive, strategic goal. The fundamental principles of the bottom-up approach can be borrowed from nature.<sup>[12–17]</sup> Biological systems provide numerous examples of micro- and nano-patterned inorganic materials that directly develop into their intricate architectures.<sup>[18–22]</sup> Their formation in biological environments is highly regulated. Different organisms, irrespective of their systematic position, exercise a level of molecular control over physico-chemical properties of minerals that is unparalleled in today’s technology. The best known yet most intriguing and fascinating natural biomineral is calcium carbonate.<sup>[18,21,23–25]</sup> Organisms control polymorph, location of nucleation, particle sizes, shapes, crystallographic orientation, composition, stability, and hierarchical assembly of this simple inorganic salt. The resulting biomaterials have elaborate, three-dimensional (3D) designs with exceptional microstructural, optical, and mechanical properties (Fig. 1).<sup>[18,22,24]</sup> From the viewpoint of materials science striving toward the development of new crystallization strategies, biological synthesis of patterned calcium carbonate structures represents an inspirational system.

Generally, the formation of biominerals is finely tuned at the molecular level by organized assemblies of specialized, organic molecules.<sup>[18–20,25–27]</sup> We can identify a number of bio-

[\*] Dr. J. Aizenberg  
Bell Laboratories/Lucent Technologies  
600 Mountain Ave, Murray Hill, NJ 07974 (USA)  
E-mail: jaizenberg@lucent.com

[\*\*] I would like to thank George Whitesides for his special involvement in this projekt. I also thank Yong-Jin Han, Andrew Black, Elia Beniash, Lia Addadi, Steve Weiner, Micha Ilan, Gretchen Lambert, David Muller, John Grazul, and Don Hamann, who all contributed significantly to this work.

mineralization principles that can be potentially applied in materials synthesis. i) Crystal nucleation is templated by membranes in the form of vesicles, syncytia, and cells, which are “primed” with specialized acidic proteins (for calcium carbonate, these are usually highly acidic sulfonated and phosphorylated proteins rich in aspartic and glutamic acids, serine

and threonine).<sup>[18,19,25–27]</sup> This interfacial molecular recognition process controls the crystallographic orientation and polymorph of the nascent biomineral.<sup>[15,28]</sup> ii) Crystal sizes, morphology, and texture are further tailored by means of ionic and soluble organic growth modifiers from solution.<sup>[28,29]</sup> iii) Another important feature of biological crystallization is

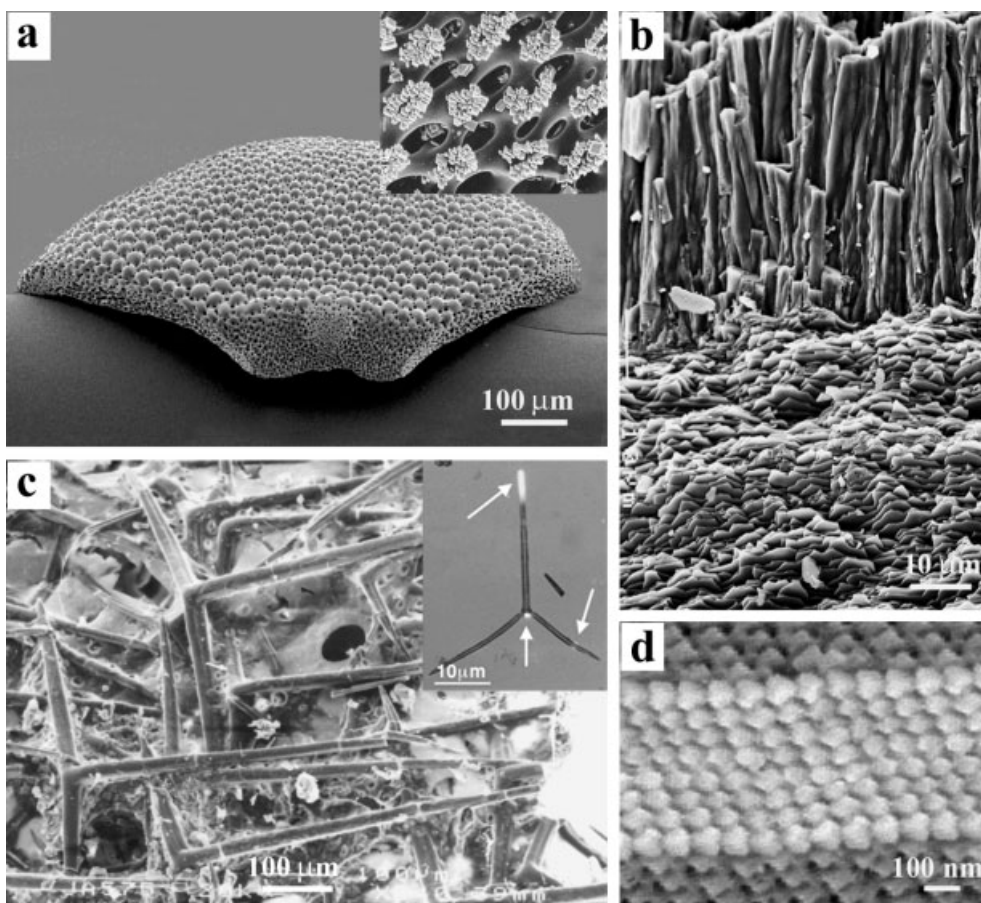


**Figure 1.** Scanning electron micrographs of biogenic calcium carbonate structures: a) Dorsal arm plate of the brittle star *Ophiocoma wendti* with the external array of microlenses. The entire elaborate structure is a single calcite crystal. The lenses are oriented in the optic axis direction of the constituent birefringent calcite. Inset: Epitaxial overgrowth of synthetic calcite crystals on a brittlestar stereom. Note that the nucleation of the newly formed calcite crystals is not homogeneous and occurs at specific, locally activated nucleation sites on the surface. b) Fragment of a mollusk shell structure showing the interface between outer prismatic (top) and inner nacreous (bottom) layer composed of arrays of single crystals of aragonite. c) Wall structure of calcareous sponge *Sycon* sp. The triradiate spicules are single crystals of calcite arranged in a regular oriented array. The orientations of their crystallographic axes bear a fixed, genetically controlled relationship to the spicule morphology. Inset: In vivo fluorescent labeling experiments show flux of ions and macromolecules to the local sites of active growth (indicated by arrows). d) Fragment of a coccolith skeleton composed of a highly periodic array of oriented, uniform nanocrystals of calcite.



*Dr. Joanna Aizenberg pursues a broad range of research interests that include biomineralization, crystal engineering, self-assembly, colloidal assembly, nanofabrication, biomaterials, optics, and biomimetics. She holds a Ph.D. in Structural Biology from the Weizmann Institute of Science. Her postdoctoral studies were carried out in George M. Whitesides group at Harvard University. Dr. Aizenberg joined Bell Laboratories in 1998, where she is working on methods for controlling various aspects of crystal formation at the nanometer scale, new micropatterning techniques, and bio-inspired optics.*

almost perfectly orchestrated control over the micro- and nano-environment of crystal nucleation and growth: biocrystals nucleate at well-defined, spatially delineated, organically modified intracellular sites and grow inside organic frameworks that confine mineral deposition within predetermined spatial patterns.<sup>[18,28,30–32]</sup> iv) Crystallization of complex structures often occurs through the transformation of a transient amorphous phase.<sup>[31–33]</sup>

Experimental approaches to controlled crystallization that were developed on the basis of the first biomineralization principle include the use of simplified molecular assemblies—Langmuir monolayers,<sup>[34–37]</sup> self-assembled monolayers (SAMs),<sup>[38–40]</sup> biological macromolecules,<sup>[12,15]</sup> synthetic polymers,<sup>[41,42]</sup> and surfactant aggregates<sup>[43,44]</sup>—as nucleation templates. These methods offered a certain level of control over crystal orientation and polymorph specificity, and showed the great potential of using supramolecular templates to regulate crystallization.

Other studies explored the second principle—solution deposition with growth modifiers, such as ions, proteins, and synthetic polymers. Calcium carbonate precipitation in the presence of various additives in solution was shown to induce the selective formation of different CaCO<sub>3</sub> polymorphs (calcite, aragonite, or vaterite), as well as the stabilization of an otherwise unstable amorphous calcium carbonate (ACC) phase.<sup>[15,21,25,45]</sup> Various additives that specifically interacted with the growing crystals were also active in controlling their morphologies and shapes.<sup>[21,26,46–48]</sup> Most of these studies, however, addressed only one “crystallization problem” at a time (e.g., oriented nucleation, polymorph specificity, or shapes of the growing crystals), and did not focus on patterned crystallization.

Recently we have developed new crystallization strategies that attempted to combine all four biomineralization principles.<sup>[49–51]</sup> The common feature of these strategies is the use of functionalized SAMs micropatterned by various soft-lithography techniques,<sup>[52,53]</sup> as spatially constrained, chemically modified microenvironments for crystallization. The power of this approach is its ability to simultaneously provide structural and molecular control of the pattern of nucleation sites on the organic template and to manipulate near-surface gradients of concentrations of the crystallizing solution at the micrometer scale. In this article, I will focus on the application of these techniques to the fabrication of arbitrary patterns of calcium carbonate crystals, and on a high level of control over multiple parameters of crystal nucleation and growth that this approach offers.

## 2. Fabrication of Regular Arrays of Uniform, Oriented Crystals

Growing an array of crystals in a predetermined pattern has proven to be a challenging feat in materials science. In contrast to the technological world, convoluted crystalline architectures composed of regularly distributed microscopic crys-

tals are typical in biological systems, with remarkable calcitic tissues being particularly prominent (Fig. 1).<sup>[18]</sup> The patterned formation of these structures is believed to be controlled *locally* by specialized macromolecules, which implies the stimulation of crystallization at certain sites and relative inhibition of the process at all other sites. The localized nucleating activity of biological molecules was demonstrated in a series of overgrowth experiments<sup>[30]</sup> (Fig. 1a, inset) and in vivo fluorescent labeling experiments<sup>[28]</sup> (Fig. 1c, inset) that mapped the regions of active nucleation and growth.

Experimental procedures outlined below originated from the above concept of using specific organic macromolecules to build the microenvironment for the localized nucleation of crystals. We chose SAMs of  $\omega$ -terminated alkanethiols as crystallization templates for a number of reasons: i) alkanethiols self-assemble on metal substrates into highly ordered, crystalline monolayers with various structural parameters,<sup>[54–56]</sup> ii) the chemistry of the interface can be modified by using  $\omega$ -functionalized alkanethiols; iii) the monolayers can be easily patterned on a submicrometer scale using various lithographic techniques. SAMs present, therefore, an attractive candidate for an organized organic surface capable of inducing the patterned crystallization.

We formed micropatterned SAMs with a controlled distribution of active nucleation sites, using two lithographic procedures: microcontact printing ( $\mu$ CP) and topographically assisted assembly. In the former approach, the SAM surface was prepared by printing a pattern of one thiol on a metal substrate using an elastomeric stamp, and filling in the bare space by another thiol (Fig. 2a).<sup>[52,53]</sup> An array of active nucleating islands or an interconnected nucleating mesh was thus generated.<sup>[50,57]</sup> In the second experimental procedure, patterned substrates were fabricated by evaporating one metal onto the surface of a second through a stencil mask or a patterned photoresist, and washing the surface with a single thiol (Fig. 2b).<sup>[49]</sup> Active nucleating sites are then formed at highly localized regions of disorder in SAMs at the edges between different metals.<sup>[49,58]</sup> The substrates were supported upside-down in a crystallization solution. We will focus on the formation of CaCO<sub>3</sub><sup>[26,30]</sup> on thus-fabricated organic substrates, although the experimental conditions and the mechanism discussed are applicable to the patterned precipitation of a wide range of inorganic and organic materials.<sup>[59–61]</sup> The terminal groups of the SAMs were chosen to correspond to the functional groups that play an important role in the biological deposition of CaCO<sub>3</sub> (A, B =  $-\text{CO}_2^-$ ,  $-\text{OH}$ ,  $-\text{SO}_3^-$ ,  $-\text{PO}_3\text{H}^-$ ,  $-\text{CH}_3$ ,  $-\text{N}(\text{CH}_3)_3^+$ ).<sup>[18,25,27]</sup> The ability to form microregions of SAMs with equivalent surface area, shape, distribution, and functionality made it possible to generate similar nucleation conditions that resulted in virtually simultaneous nucleation in different locations. The templated crystals were, therefore, of uniform size and nucleation density over large patterned areas. The produced patterned calcitic films followed the underlying organic patterns with high fidelity.<sup>[49,50,54,55]</sup>

In previous studies, we showed that the localized crystallization on patterned SAMs could be explained in terms of diffu-

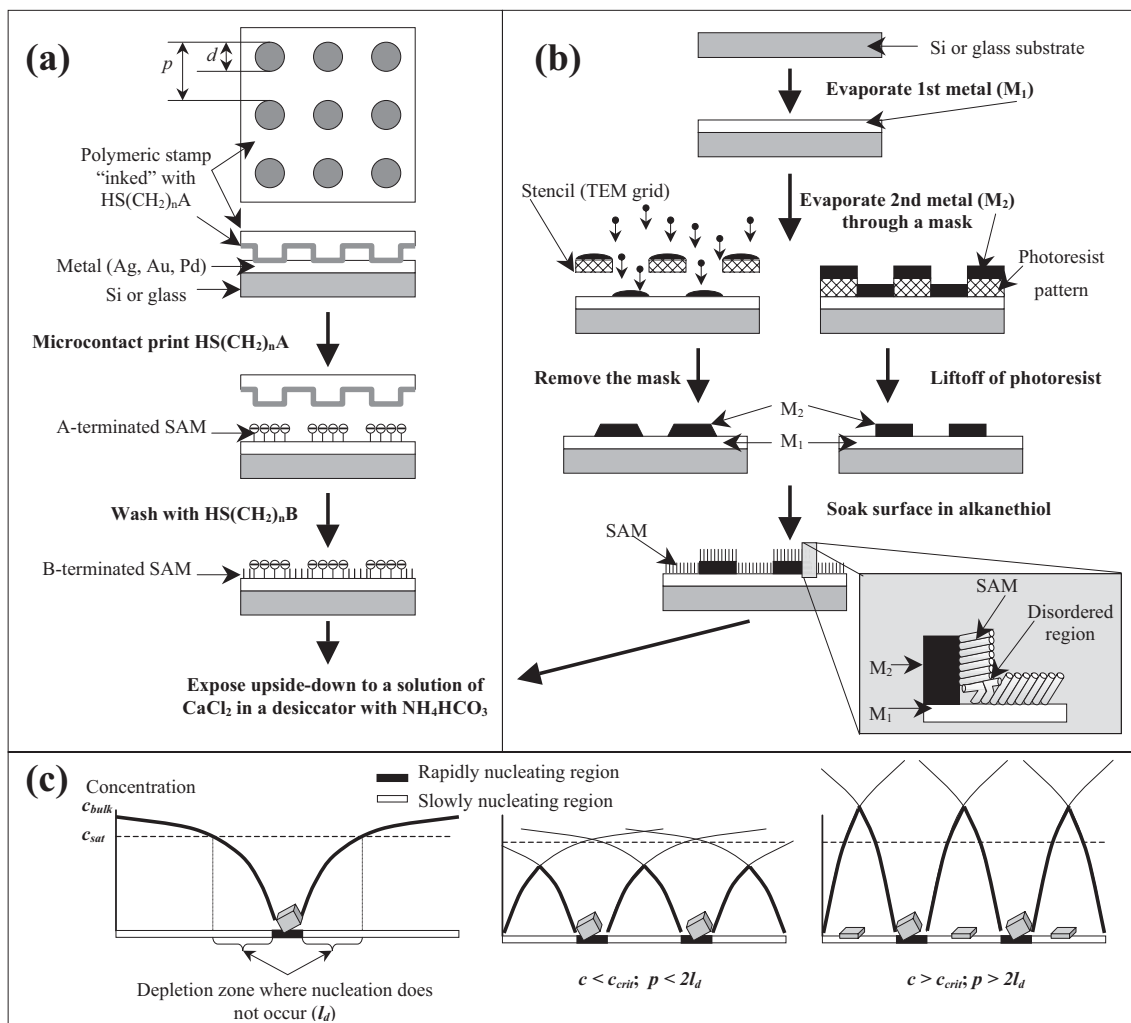


**Figure 2.** Schematic illustration of the experimental steps for the fabrication of micropatterned substrates used in the crystal growth experiments: a) microcontact printing; b) topographically assisted self-assembly; and c) mechanism of localized crystal growth.

sion-limited, island-specific nucleation.<sup>[50,58,62]</sup> When the organic substrate is patterned with regions of different nucleating activity, nucleation begins at rapidly nucleating sites and induces the ion flux into these regions, which depletes the solution over slowly nucleating regions. In the zone  $l_d$  where the effective concentration of the solution is below saturation ( $c_{sat}$ ), nucleation does not occur. Therefore, if we keep the distance between rapidly nucleating regions below  $2l_d$ , crystallization is entirely restricted to the rapidly nucleating regions (Fig. 2c).

The modification of various parameters of the experimental setup—the functional groups and the length of the SAM(s), the supporting metal/metals combination, the concentration and composition of the crystallizing solution, the density and sizes of the features in the stamp—makes it possible to exert high level of control over many of the crucial aspects of nucleation and crystal growth. In addition to precise localization of nucleation, we can regulate the density of the active nucleating regions on the surface ( $N$ , [ $\text{mm}^{-2}$ ]), the number of crystals

that nucleate within each region ( $n$ ), crystal polymorph, morphology, and crystallographic orientation.

High-resolution patterns of uniform, oriented calcium carbonate crystals were generally fabricated using the following algorithm. a) We choose a specific SAM/metal combination that induces the formation of a desired polymorph<sup>[63]</sup> and its oriented nucleation.<sup>[64–66]</sup> b) In  $\mu\text{CP}$  experiments, for a given  $N$ , we determine the corresponding distance between the features in the stamp,  $p$  (Fig. 2a, top):  $p = N^{-0.5}$ . c) By varying the concentration of the crystallizing solution, we define the range of concentrations ( $c_{bulk} < c_{crit}$ , for which  $l_d > p/2$ ). d) In  $\mu\text{CP}$  experiments, the number of crystals,  $n$ , within each active nucleation region appeared to depend linearly upon its area.<sup>[50,57]</sup> The latter relationship makes it possible to determine the optimum size,  $d$ , of the raised features in the stamp (Fig. 2a, top) for any chosen  $n$ . e) Crystal morphology is then modulated by the addition of specific growth modifiers to the crystallizing solution.<sup>[67]</sup>

A variety of thus fabricated patterned calcium carbonate films is shown in Figure 3. When  $c < c_{crit}$ , the crystals can be

grown in dense islands (Fig. 3a) or in ordered two-dimensional arrays of isolated single crystals of uniform size, orientation, and morphology (Figs. 3b,c). We can reverse the crystallization pattern and fabricate interconnected mineral films (Fig. 3d,e). Calcitic outlines the underlying disordered interfaces formed on SAMs supported on mixed metal substrates (Fig. 3f). Using  $c > c_{\text{crit}}$ , we fabricated complex patterned films comprising the combination of two  $\text{CaCO}_3$  polymorphs (Fig. 3g) or crystals of the same polymorph grown in different crystallographic orientations (Fig. 3h).

### 3. Bottom-Up Synthesis of Large Micropatterned Single Crystals

Fabrication of crystallographically oriented single crystals with regular micrometer- and nanometer-sized features presents another materials challenge. These crystals are broadly used in technology as components of various electronic, optical, and sensory devices. Learning from nature and introducing biological crystal growth techniques could potentially improve the complex technological processing routes currently used for patterning single crystals. An inspirational biological system is single crystals of calcite formed by echino-

derms.<sup>[18]</sup> Figure 1a shows a brittlestar arm plate: the entire element with its micrometer feature sizes is a unique, intricately shaped, single-crystalline, 3D meshwork (so-called stereom) bearing an array of highly efficient microlenses with controlled orientation of the optical axis of the constituent calcite.<sup>[24]</sup> This structure represents a fascinating example of a multifunctional biomaterial that effectively fulfills mechanical and optical functions. The mechanism of the formation of such structures is still a mystery. It has been shown, however, that in certain biological systems, crystallization takes place through the transformation of a transient metastable ACC phase triggered by regiospecific, oriented nucleation.<sup>[31–33]</sup> Figure 4 depicts such an amorphous-to-crystalline transition in a sea urchin larval spicule.

For the purposes of bio-inspired crystal engineering, we identified two major elements of the sea urchin larval spicule formation and used them in our synthetic effort: i) Amorphous calcium carbonate stabilized by specialized macromolecules is deposited in a preformed space and adopts its shape. ii) Oriented nucleation then occurs at a well-defined, chemically modified intracellular site and the crystallization front propagates through the amorphous phase, resulting in the formation of a single crystal with controlled orientation and predetermined microstructure.<sup>[31]</sup> We have shown that biogenic ACC is stabilized by means of specialized macromolecules

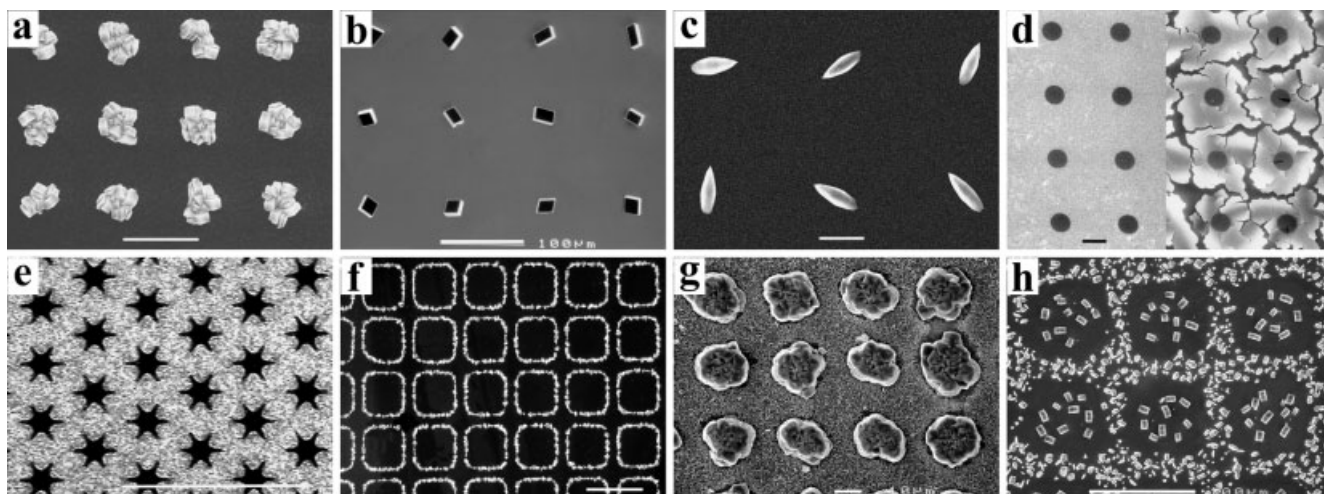


**Figure 3.** Examples of micropatterned, oriented  $\text{CaCO}_3$  films formed on the SAM templates. The substrates in (a–e) and (g) were fabricated by  $\mu\text{CP}$  (see Fig. 2a); the substrates in (f,h) were fabricated using topographically assisted assembly (see Fig. 2b): a) Square array of polycrystalline calcitic islands formed on SAMs of  $\text{HS}(\text{CH}_2)_{15}\text{CO}_2\text{H}$  supported on Au.  $\text{CH}_3$ -terminated thiol was used as the background. Crystals grew selectively from the (015) nucleating plane.  $N = 10\,000$ ;  $n \sim 12$ . b) Square array of discrete single crystals of calcite formed on SAMs of  $\text{HS}(\text{CH}_2)_{22}\text{OH}$  supported on Au.  $\text{CH}_3$ -terminated thiol was used as the background. Crystals grew selectively from the (104) nucleating plane.  $N = 100$ ;  $n = 1$ . c) Array of needle-like crystals of modified morphology was formed in the presence of Mg ion in solution [67]. The substrate consisted of  $\text{CO}_2\text{H}$ - and  $\text{CH}_3$ -terminated thiol supported on Ag. Crystals grew selectively from the (012) nucleating plane.  $N = 1000$ ;  $n = 1$ . d) Interconnected, patterned ACC film (left) formed on a disordered SAM that consisted of a mixture of thiol molecules of different lengths terminated in phosphate, hydroxyl, and methyl groups. The film transformed into a patterned crystalline calcitic layer (right). e) Micropatterned, polycrystalline calcitic film with “snowflake” holes. The edge resolution is  $< 50$  nm. f) Calcite growth on a SAM of  $\text{HS}(\text{CH}_2)_{15}\text{CO}_2\text{H}$  supported on a mixed Au/Ag substrate fabricated using TEM grid as a mask. Crystals selectively grew at the disordered regions in the SAM formed at the interfaces between the two metals. g) Patterning of two  $\text{CaCO}_3$  polymorphs, calcite and vaterite, from a highly saturated  $\text{CaCl}_2$  solution. The substrate consisted of islands of  $\text{SO}_3\text{H}$ -terminated SAMs in  $\text{N}(\text{CH}_3)_3^+$ -terminated background supported on Au. Calcite crystals selectively grew on  $\text{SO}_3\text{H}$ -terminated SAMs, while vaterite decorated the  $\text{N}(\text{CH}_3)_3^+$ -terminated areas. h) Calcite growth in two different crystallographic orientations on a SAM of  $\text{HS}(\text{CH}_2)_{15}\text{CO}_2\text{H}$  supported on a mixed Au/Ag substrate fabricated using TEM grid as a mask. Highly saturated  $\text{CaCl}_2$  solution was used. On the Au islands, crystals nucleated selectively from the (015) plane; on the Ag background crystals nucleated selectively from the (012) plane. Scale bars in (a,c,d,g) are 10  $\mu\text{m}$ ; in (b,e–h) they are 100  $\mu\text{m}$ .

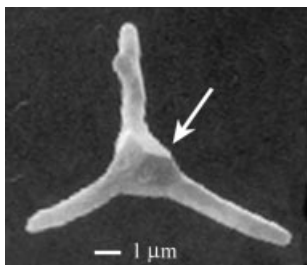


**Figure 4.** Sea urchin *Paracentrotus lividus* larval spicule (25 h embryo). Triradiate spicule is first deposited in the ACC form within a membrane-delineated compartment, inside a syncytium formed by specialized mesodermal cells. Within 20 h, an oriented calcite with the crystallographic *a*-axes parallel to the three radii nucleates in the center of a spicule (see the rhombohedral-shaped crystal indicated by an arrow). The subsequent amorphous-to-crystalline transition results in the formation of a single crystal of calcite that has the predetermined triradiate shape and constant crystallographic orientation [31,32].

rich in hydroxyamino acids, glycine, glutamate, phosphate, and polysaccharides.<sup>[25]</sup> These macromolecules extracted from the biological ACC tissue and introduced as an additive into saturated calcium carbonate solution induced the formation of stabilized ACC in vitro. The stabilization of ACC can also be achieved using surface-mediated processes. Our results show that significantly disordered organic substrates bearing phosphate and hydroxyl groups, suppress the nucleation of calcite, and induce the formation of a metastable ACC layer from highly saturated solutions.<sup>[51]</sup> The deposited ACC layer is stabilized for 1–2 h and then transforms into a polycrystalline film (Fig. 3d).

Experimental procedures that were designed on the basis of the above biomineralization principles are shown in Figure 5.<sup>[51]</sup> The micropatterned 3D substrate was primed with a disordered phosphate-, methyl-, and hydroxy-terminated monolayer that induces the formation of amorphous CaCO<sub>3</sub>. One nanoregion of a SAM of HS(CH<sub>2</sub>)<sub>n</sub>A (A=OH, CO<sub>2</sub>H, SO<sub>3</sub>H) serving as calcite nucleation site was integrated into each template (Fig. 5a). When placed in a supersaturated solution of calcium carbonate, these organically modified templates induced the deposition of the ACC mesh in the interstices of the framework (Fig. 5b). Oriented nucleation of calcite then occurred at the SAM nanoregion, followed by the propagation of the crystallization front through the ACC film. The resulting crystal preserves the shape of the “perforated” ACC film, and its orientation is determined by the SAM nucleation site. This new bio-inspired crystal engineering strategy made it possible to directly fabricate millimeter-sized single crystals with a predetermined sub-10 μm pattern and crystallographic orientation (Fig. 6).

Control crystallization experiments aimed at elucidating the mechanism of the amorphous-to-crystalline transition were performed using 3D templates engineered with or without nucleation sites, with varied feature sizes and using impurities in the solution. These experiments suggested that organically modified 3D templates with the feature sizes smaller than 10 μm, in addition to stabilizing the ACC and to controlling

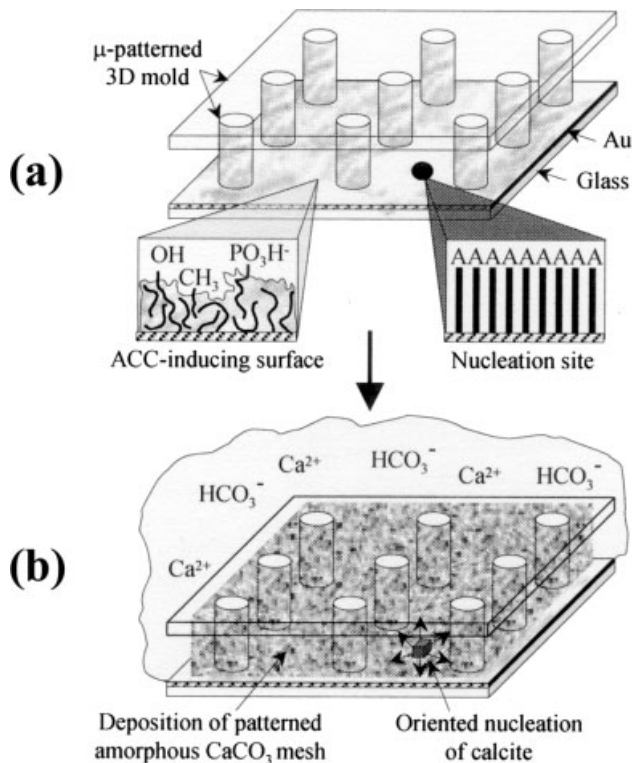


**Figure 5.** Schematic of the new approach that leads to the formation of “microperforated” single crystals: a) structural and chemical features of the engineered 3D templates; b) deposition of the ACC mesh from the CaCO<sub>3</sub> solution, followed by the oriented nucleation at the imprinted nucleation site and the amorphous-to-crystalline transition of the ACC film.

the oriented crystal nucleation and the micropattern of the single crystal, also act as stress release sites and discharge sumps for excess water and impurities during crystallization.

The use of the concept of the amorphous-to-crystalline transition within functionalized micropatterned templates may have important generic implications in materials science. The possible applications of the engineered 3D frameworks may include the direct growth of defect-free micropatterned crystals, the relaxation of stresses encountered during amorphous-to-crystalline transitions in existing materials, controlled solvent release during polycondensation reactions, etc.<sup>[10,11,68]</sup>

Interestingly, the achievable size range of the mesh in synthetic calcite crystals is comparable with the stereom sizes in their biologically formed counterparts. This observation suggests that the described mechanisms of the amorphous-to-crystalline transition may also have direct biological relevance. It is conceivable that a 3D array of self-assembling biological macromolecules and/or cells serving as structural templates will provide sites for stress relaxation and impurity discharge during amorphous-to-crystalline transition, thus giving rise to the formation of a large microporous single crystal.

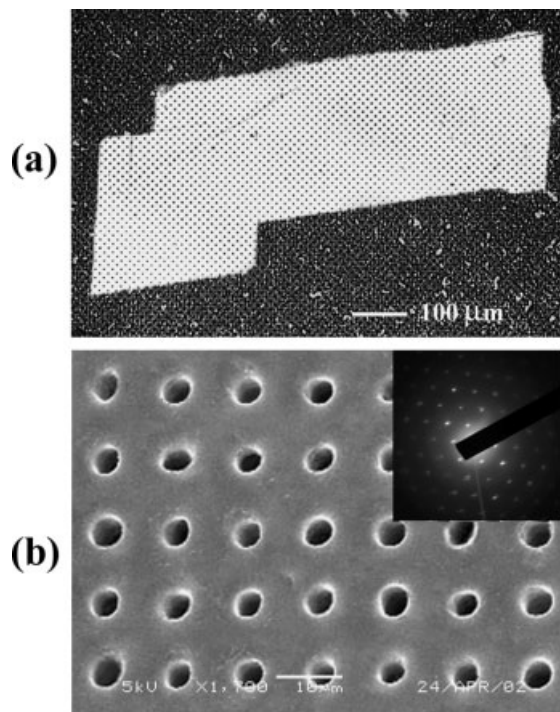


**Figure 6.** Micropatterned synthetic calcite crystal formed within chemically modified 3D templates using the “amorphous-to-crystalline transition” approach: a) polarized light micrograph, showing the perforated single crystal of calcite with the feature sizes of  $\sim 10 \mu\text{m}$  and the polycrystalline background. b) Magnified scanning electron micrograph of the crystal, showing its regular microstructure. Inset: a large-area transmission electron diffraction pattern, confirming that the section is a single crystal of calcite oriented along the optic axis.

#### 4. Concluding Remarks

Ordered crystalline films are critical materials for various technological and biomedical applications. The development of new methods of the pattern generation on a sub-micrometer scale is, therefore, a challenging problem in crystal engineering. In this article, I have shown that high level of control over inorganic crystallization could be achieved using supra-molecular crystallization templates, which are composed of SAMs micropatterned by soft-lithography techniques. The power of the presented bio-inspired approaches to artificial crystallization is based on the ability to govern mass transport to different regions of the surface at a micrometer scale and to tune the molecular structure and microenvironment of the nucleation site by patterning  $\omega$ -terminated SAMs into regions with different nucleating activity. Using crystallization of calcite as an example, it has been demonstrated that SAMs control various aspects of the crystallization process and provide means to fabricate arbitrarily patterned crystalline structures (regular arrays of uniform oriented crystals, oriented polycrystalline films and large, microporous single crystals).

Natural crystalline materials with their sophisticated architectures and micrometer-scale regularity provide an unlimited

source of inspiration and concepts for the rational design of artificial crystalline materials. It is believed that biological principles, if understood correctly and creatively applied in technology, could well revolutionize our ability to control crystallization. Such bottom-up fabrication of inorganic solids with micrometer-scale regularity and exquisite ornamentation could offer the exciting prospect of applications in the synthesis of new materials with optimized mechanical, optical, electric, and catalytic performance. The information acquired in biomimetic experiments may also shed light on basic biomineralization mechanisms.

Received: April 15, 2004

- [1] A. H. Heuer, D. J. Fink, V. J. Laraia, J. L. Arias, P. D. Calvert, K. Kendall, G. L. Messing, J. Blackwell, P. C. Rieke, D. H. Thompson, A. P. Wheeler, A. Veis, A. I. Caplan, *Science* **1992**, *255*, 1098.
- [2] C. B. Murray, C. R. Kagan, M. G. Bawendi, *Science* **1995**, *270*, 1335.
- [3] S. I. Stupp, P. V. Braun, *Science* **1997**, *277*, 1242.
- [4] *Better Ceramics Through Chemistry* (Eds: B. J. J. Zelinsky, C. J. Brinker, D. E. Clark, D. R. Ulrich), Materials Research Society, Pittsburgh, PA **1990**.
- [5] S. Mann, G. A. Ozin, *Nature* **1996**, *382*, 313.
- [6] C. J. Brinker, *Curr. Opin. Solid State Mater. Sci.* **1996**, *1*, 798.
- [7] F. Schüth, W. Schmidt, *Adv. Mater.* **2002**, *14*, 629.
- [8] T. W. Odom, J. L. Huang, P. Kim, C. M. Lieber, *Nature* **1998**, *391*, 62.
- [9] D. Zhao, P. Yang, N. Melosh, J. Feng, B. F. Chmelka, G. D. Stucky, *Adv. Mater.* **1998**, *10*, 1380.
- [10] *Nucleation and Growth Processes in Materials* (Ed: A. Gonis), Materials Research Society, Boston, MA **2000**.
- [11] A. W. Vere, *Crystal Growth: Principles and Progress, Updates in Applied Physics and Electrical Technology*, Plenum, New York **1988**.
- [12] L. Addadi, S. Weiner, *Proc. Natl. Acad. Sci. USA* **1985**, *82*, 4110.
- [13] *Materials Synthesis Based on Biological Processes* (Eds: M. Alper, P. D. Calvert, R. Frankel, P. C. Rieke, D. A. Tirrell), Materials Research Society, Pittsburgh, PA **1991**.
- [14] *Biomimetic Materials Chemistry* (Ed: S. Mann), VCH, New York **1996**.
- [15] A. M. Belcher, R. J. Christensen, P. K. Hansma, G. D. Stucky, D. E. Morse, *Nature* **1996**, *381*, 56.
- [16] S. Mann, *Nature* **1993**, *365*, 499.
- [17] I. A. Aksay, M. Trau, S. Manne, I. Honma, N. Yao, L. Zhou, P. Fenter, P. M. Eisenberger, S. M. Gruner, *Science* **1996**, *273*, 892.
- [18] H. A. Lowenstam, S. Weiner, *On Biomineralization*, Oxford University Press, New York **1989**.
- [19] *Biomineralization. Chemical and Biological Perspectives* (Eds: S. Mann, J. Webb, R. J. P. Williams), VCH, Weinheim, Germany **1989**.
- [20] L. Addadi, S. Weiner, *Angew. Chem. Int. Ed. Engl.* **1992**, *31*, 153.
- [21] L. Addadi, S. Raz, S. Weiner, *Adv. Mater.* **2003**, *15*, 959.
- [22] S. A. Wainwright, W. D. Biggs, J. D. Currey, J. M. Gosline, *Mechanical Design in Organisms*, John Wiley, New York **1976**.
- [23] F. Lippmann, *Sedimentary Carbonate Minerals*, Springer, Berlin, Germany **1973**.
- [24] J. Aizenberg, A. Tkachenko, S. Weiner, L. Addadi, G. Hendler, *Nature* **2001**, *412*, 819.
- [25] J. Aizenberg, G. Lambert, S. Weiner, L. Addadi, *J. Am. Chem. Soc.* **2002**, *124*, 32.
- [26] S. Albeck, J. Aizenberg, L. Addadi, S. Weiner, *J. Am. Chem. Soc.* **1993**, *115*, 11 691.
- [27] S. Weiner, L. Addadi, *Trends Biochem. Sci.* **1991**, *16*, 252.
- [28] J. Aizenberg, M. Ilan, S. Weiner, L. Addadi, *Connect. Tissue Res.* **1996**, *34*, 255.

- [29] A. Berman, J. Hanson, L. Leiserowitz, T. F. Koetzle, S. Weiner, L. Addadi, *Science* **1993**, 259, 776.
- [30] J. Aizenberg, S. Albeck, S. Weiner, L. Addadi, *J. Cryst. Growth* **1994**, 142, 156.
- [31] E. Beniash, J. Aizenberg, L. Addadi, S. Weiner, *Proc. R. Soc. London Ser. B* **1997**, 264, 461.
- [32] E. Beniash, L. Addadi, S. Weiner, *J. Struct. Biol.* **1999**, 125, 50.
- [33] I. M. Weiss, N. Tuross, L. Addadi, S. Weiner, *J. Exp. Zool.* **2002**, 293, 478.
- [34] E. M. Landau, M. Levanon, L. Leiserowitz, M. Lahav, J. Sagiv, *Nature* **1985**, 318, 353.
- [35] X. K. Zhao, J. H. Fendler, *J. Phys. Chem.* **1991**, 95, 3716.
- [36] S. Mann, B. R. Heywood, S. Rajam, J. D. Birchall, *Nature* **1988**, 334, 692.
- [37] P. W. Carter, M. D. Ward, *J. Am. Chem. Soc.* **1993**, 115, 11 521.
- [38] B. C. Bunker, P. C. Rieke, B. J. Tarasevich, A. A. Campbell, G. E. Fryxell, G. L. Graff, L. Song, J. Liu, J. W. Virden, G. L. McVay, *Science* **1994**, 264, 48.
- [39] S. Feng, T. Bein, *Nature* **1994**, 368, 834.
- [40] V. K. Gupta, N. L. Abbott, *Science* **1997**, 276, 1533.
- [41] A. Berman, D. J. Ahn, A. Lio, M. Salmeron, A. Reichert, D. Char-ych, *Science* **1995**, 269, 515.
- [42] J. D. Hartgerink, E. Beniash, S. I. Stupp, *Science* **2001**, 294, 1684.
- [43] D. D. Archibald, S. Mann, *Nature* **1993**, 364, 430.
- [44] T. Douglas, D. P. E. Dickson, S. Betteridge, J. Charnock, C. D. Garner, S. Mann, *Science* **1995**, 269, 54.
- [45] G. Falini, S. Albeck, S. Weiner, L. Addadi, *Science* **1996**, 271, 67.
- [46] C. A. Orme, A. Noy, A. Wierzbicki, M. T. McBride, M. Granthan, H. H. Teng, P. M. Dove, J. J. Deyoreo, *Nature* **2001**, 411, 775.
- [47] S. H. Yu, H. Colfen, M. Antonietti, *J. Phys. Chem. B* **2003**, 107, 7396.
- [48] J. J. M. Donners, R. J. M. Nolte, N. A. J. M. Sommerdijk, *J. Am. Chem. Soc.* **2002**, 124, 9700.
- [49] J. Aizenberg, A. J. Black, G. M. Whitesides, *Nature* **1998**, 394, 868.
- [50] J. Aizenberg, A. J. Black, G. M. Whitesides, *Nature* **1999**, 398, 495.
- [51] J. Aizenberg, D. A. Muller, J. L. Grazul, D. R. Hamann, *Science* **2003**, 299, 1205.
- [52] A. Kumar, N. A. Abbott, E. Kim, H. A. Biebuyck, G. M. Whitesides, *Acc. Chem. Res.* **1995**, 28, 219.
- [53] Y. Xia, G. M. Whitesides, *Angew. Chem. Int. Ed.* **1998**, 37, 550.
- [54] R. G. Nuzzo, L. H. Dubois, D. L. Allara, *J. Am. Chem. Soc.* **1990**, 112, 558.
- [55] P. E. Laibinis, G. M. Whitesides, D. L. Allara, Y. T. Tao, A. N. Parikh, R. G. Nuzzo, *J. Am. Chem. Soc.* **1991**, 113, 7152.
- [56] P. E. Laibinis, G. M. Whitesides, *J. Am. Chem. Soc.* **1992**, 114, 1990.
- [57] J. Aizenberg, *J. Cryst. Growth* **2000**, 211, 143.
- [58] J. Aizenberg, *J. Chem. Soc., Dalton Trans.* **2000**, 3963.
- [59] F. C. Meldrum, J. Flath, W. Knoll, *Thin Solid Films* **1999**, 348, 188.
- [60] M. Bartz, A. Terfort, W. Knoll, W. Tremel, *Chem. Eur. J.* **2000**, 6, 4149.
- [61] C. C. Chen, J. J. Lin, *Adv. Mater.* **2001**, 13, 136.
- [62] A.-L. Barabási, H. E. Stanley, *Fractal Concepts in Surface Growth*, Cambridge University Press, Cambridge, UK **1995**.
- [63] J. Küther, R. Seshadri, W. Knoll, W. Tremel, *J. Mater. Chem.* **1998**, 8, 641.
- [64] J. Aizenberg, A. J. Black, G. M. Whitesides, *J. Am. Chem. Soc.* **1999**, 121, 4500.
- [65] Y.-J. Han, J. Aizenberg, *Angew. Chem. Int. Ed.* **2003**, 42, 3668.
- [66] A. M. Travaille, L. Kaptijn, P. Verwer, B. Hulsken, J. A. A. W. Elemans, R. J. M. Nolte, H. van Kempen, *J. Am. Chem. Soc.* **2003**, 125, 11 571.
- [67] Y.-J. Han, J. Aizenberg, *J. Am. Chem. Soc.* **2003**, 125, 4032.
- [68] T. P. Leervad Pedersen, J. Kalb, W. K. Njoroge, D. Wamwangi, M. Wuttig, F. Spaepen, *Appl. Phys. Lett.* **2001**, 79, 3597.